Analytical Chemistry: A Journal (2024)
Clausius Scientific Press, Canada

DOI: 10.23977/analc.2024.030112
ISSN 2616-1958 Vol. 3 Num. 1

Study on wet corrosion removal of InAsSb focal plane device substrate

Qiang Li[1,a,*]

[1]*Anhui Guangzhi Technology Co, Chuzhou, Anhui, China*
[a]*18815614113@163.com*
[*]*Corresponding author*

Keywords: InAsSb; GaSb substrate; Backside corrosion

Abstract: A highly selective corrosion solution has been developed, capable of completely dissolving the GaSb substrate of InAsSb focal plane devices. This solution effectively mitigates the absorption of infrared radiation and the detrimental effects associated with the mechanical thinning of the focal plane device substrate. The study focused on the CrO_3 series, wherein the concentrations of CrO_3 and H_3PO_4 in the solution were systematically varied to assess their impact on the corrosion of InAsSb and GaSb materials. The extent of corrosion was quantitatively evaluated using a step meter and a 3D profilometer. The experimental results yielded an optimal solution ratio, resulting in a corrosion rate of 173 nm/s for GaSb, while InAsSb exhibited negligible corrosion. The surface roughness of GaSb was reduced from S_a = 1.2853 nm prior to corrosion to S_a = 1.0679 nm following treatment with the optimal solution ratio. Subsequent to packaging, the focal plane chip was tested at a temperature of 150K, revealing that the corrosion process effectively eliminated surface damage. The average response voltage recorded for the device was 553 mV, with an average noise equivalent temperature difference (NETD) of 20.98 mK. Notably, the performance of the focal plane device remained unaffected post-corrosion. This research holds significant implications for the advancement of back corrosion technology in InAsSb focal plane devices.

1. Introduction

Infrared detection technology is extensively utilized across military, aerospace, and medical sectors. Central to infrared detectors are various optical components, with the focal plane chip serving as the primary element responsible for the absorption of infrared radiation. This chip employs the photoelectric effect to transform the absorbed radiation into an electrical signal via the readout circuit facilitated by flip-flop interconnections [1]. The expanding range of applications for infrared detectors has led to increasingly stringent requirements, with a focus on developing detectors that are compact, lightweight, and energy-efficient being paramount for future advancements [2-3]. Notably, detectors made from mercury cadmium telluride and indium antimonide necessitate refrigeration to maintain optimal operating conditions, resulting in high power consumption and larger physical dimensions. Furthermore, the production costs associated with mercury cadmium telluride are exacerbated by challenges related to material growth and defects, while the wavelength tuning of indium antimonide

presents significant difficulties, both of which pose challenges for the future development of these technologies [4-5].

InAsSb is classified as a III-V compound semiconductor material, specifically a direct bandgap semiconductor. By varying the antimony (Sb) content, it is possible to achieve detection capabilities within the 3-12 μm wavelength range. This material exhibits a long carrier lifetime, a high absorption coefficient, and elevated carrier mobility, maintaining significant sensitivity and detection rates even at a temperature of 150K[6]. Consequently, InAsSb represents a pivotal area of research for future advancements in detector miniaturization, low power consumption, and high sensitivity.

The introduction of nBn-type devices in 2006 marked a significant development in this field, wherein a barrier layer is incorporated during the material growth process. This barrier layer, characterized by a wide bandgap, effectively mitigates the depletion region associated with narrow bandgap semiconductors. By obstructing the majority carriers, the barrier layer minimizes the generation of compound current, thereby reducing the dark current linked to the depletion region and enhancing the operational temperature of the detector[7].

InAsSb material is typically synthesized using molecular beam epitaxy on a GaSb substrate[8]. This method allows for precise control over the growth process, resulting in large material sizes with minimal defects. The fabrication of the focal plane is accomplished through a series of processes including photolithography, etching, metallization, and inverted welding. However, the GaSb substrate exhibits significant absorption of infrared light, which adversely impacts the imaging quality of the detector. Additionally, the thermal expansion coefficient differences during the operational hot and cold switching of the detector can induce stress, leading to the formation of lobes. To enhance the reliability, stability, and longevity of the detector focal planes, it is essential to thin the substrate material prior to the completion of the device packaging tests. This thinning process aims to reduce the substrate's infrared radiation absorption. Commonly employed substrate thinning techniques involve initial diamond single-point removal to eliminate the majority of the substrate, followed by mechanical chemical abrasion or the application of a relatively low concentration corrosion etching solution for further thinning of the remaining substrate. However, mechanical chemical abrasion does not entirely mitigate the damage caused by mechanical actions, as illustrated in Figure 1, which can subsequently affect the imaging quality and yield during chip production[9-10]. Furthermore, even after employing a low concentration corrosion solution, the remaining substrate continues to absorb infrared radiation, thereby compromising the imaging performance of infrared detectors. Additionally, these methods do not fully address the stress effects that may arise between the substrate and the epitaxial layer due to differences in thermal expansion coefficients.

Figure 1: Level map with damage on the device surface

This study addresses the damage incurred during the mechanical processing of InAsSb focal plane substrates and aims to achieve complete substrate removal through a corrosion solution specifically designed for GaSb. The research examines the variations in the composition ratios of the corrosion

solution, as well as the characterization of the corroded surfaces utilizing metallurgical microscopy, step measurement techniques, and three-dimensional profiling. The findings indicate the selection of a corrosion solution that effectively removes GaSb substrates, characterized by high specific gravity, favorable morphology, and rapid corrosion rates. Additionally, the performance evaluation of the focal plane post-substrate removal is emphasized, highlighting its significance in the context of InAsSb focal plane substrate processing.

2. Experimental

The InAsSb focal plane array examined in this study features a resolution of 640×512 pixels, with a deep table structure characterized by an etching depth ranging from 3.9 to 4.1 μm, and an individual pixel size of 15×15 μm. The InAsSb material for the focal plane array is synthesized using molecular beam epitaxy (MBE) on a GaSb substrate. The configuration and thickness of the epitaxial layers are detailed in Table 1. The growth process begins with the deposition of a GaSb transition layer, followed by the InAsSb barrier layer, the InAsSb absorber and barrier layer, and concludes with the InAsSb top electrode contact layer.

Subsequent to the growth of the epitaxial material, it is integrated with the readout circuit through a series of processes including photolithography, etching, passivation, metallization, and scribing. The substrate thickness is subsequently reduced to 25-30 μm via single-point thinning. Prior to substrate removal, the readout circuit pads are safeguarded using photoresist, after which the substrate is subjected to an etching process.

Table 1: Structure of the epitaxial layers described

framework	Thickness/nm
(1) InAsSb	100
(2) InAsSb	150
(3) InAs/AlSb	150
(4) InAsSb	3500
(5) InAsSb	500
(6) GaSb buffer	200

The primary constituents of the initial corrosion solution were chromium trioxide (CrO_3) and hydrofluoric acid (HF). An investigation was conducted to assess the influence of CrO_3 concentration on the corrosion rates of indium arsenide antimonide (InAsSb) and gallium antimonide (GaSb), with the aim of identifying the optimal CrO_3 concentration. Following the determination of this optimal concentration, the effect of phosphoric acid (H_3PO_4) content on the corrosion rates of InAsSb and GaSb was subsequently examined. This led to the establishment of the optimal ratio of the corrosion solution. The identified optimal ratio was then employed to facilitate the removal of the backside substrate of the InAsSb focal plane chip subsequent to single-point thinning. Upon completion of the corrosion process, a three-dimensional profiler was utilized to assess the condition of the backside substrate of the InAsSb focal plane. The corrosion solution ratio was optimized for the removal of the backside substrate corrosion on the InAsSb focal plane chip, and a comparative analysis of the surface state before and after corrosion was conducted. Subsequently, the InAsSb focal plane device was encapsulated in a Dewar and evaluated for photovoltaic performance at a temperature of 150 K. The corrosion rate was ascertained based on the H_3PO_4 content, ultimately leading to the determination of the optimal corrosion solution ratio.

3. Experimental results and analysis

3.1. Effect of CrO_3 content on the corrosion rates of GaSb and InAsSb

The experimental setup involves varying the ratio of chromium trioxide (CrO_3) to hydrofluoric acid (HF) in the solution, specifically maintaining the ratio as CrO_3:HF = x:1, where x can take values of 1, 2, 3, 4, or 5. A specific volume of water is added to facilitate the dissolution of the components, resulting in five distinct corrosion solutions, labeled A, B, C, D, and E. The procedure begins with weighing CrO_3 in a polytetrafluoroethylene (PTFE) beaker, followed by the addition of water to dissolve the CrO_3. Subsequently, HF is introduced, and the mixture is stirred thoroughly before being allowed to stand for 10 minutes.

In the next phase, several samples of gallium antimonide (GaSb) and indium antimonide (InAsSb) are prepared. Half of each sample is coated with photoresist, as illustrated in Figure 2, and then baked at 90 ℃ for 10 minutes. The samples are subsequently immersed in the various corrosion solutions for a duration of 5 minutes. After corrosion, the samples are rinsed in an overflow pool to remove any residual solution, followed by the application of acetone and ethanol to eliminate the photoresist. The samples are then dried using a nitrogen gas gun.

For each corrosion solution, three slices of each material are subjected to the corrosion process. The height difference between the exposed (corroded) areas and the protected areas is measured using a step meter. The average height difference is calculated, and the corrosion rate is determined by dividing this average height difference by the corrosion time.

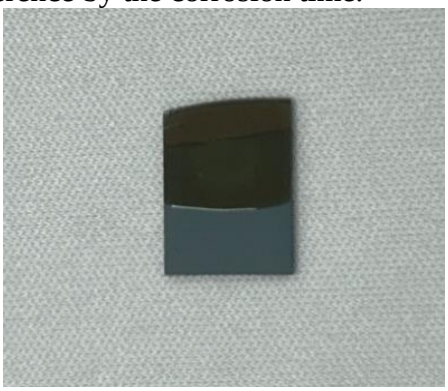

Figure 2: Corrosive materials

Chromium trioxide (CrO_3), when dissolved in water, produces chromic acid, which exhibits significant oxidizing properties, surpassing those of hydrofluoric acid (HF). In the corrosion process, chromic acid functions as an oxidant, initially oxidizing gallium antimonide (GaSb) to form gallium oxide (Ga_2O_3) and antimony oxide (Sb_2O_3). Both of these oxides are poorly soluble in water and tend to adhere to the material's surface. HF serves as a corrosive agent, facilitating the complexation reaction that generates soluble species, thereby promoting uniform corrosion of the material and enabling the dissolution of the corroded material[11].

Table 2 presents the corrosion rates of GaSb materials in solutions with varying proportions. As the concentration of CrO_3 increases, the corrosion rate of the GaSb solution initially rises and subsequently declines. The maximum corrosion rate of 43.3 nm/s occurs at a CrO_3 concentration of x = 3. Beyond this point, further increases in CrO_3 concentration lead to a decrease in the corrosion rate. The dissolution of CrO_3 in water results in the formation of chromic acid, which acts as an oxidizing agent, while HF contributes to the decomposition of complexes. At lower concentrations of CrO_3, the oxidation reaction proceeds slowly, and the corrosion rate is primarily governed by the oxidation process. Conversely, as the CrO_3 concentration increases, the rate of oxidation also rises,

allowing the oxidized material to be solubilized by HF complexes, thus increasing the corrosion rate.

However, when the concentration of CrO_3 is excessively high, the amount of HF may become insufficient to facilitate timely complexation and decomposition of the oxidized materials. This delay in complexation can hinder further oxidation, resulting in a corrosion rate that is influenced by the stages of complexation and decomposition. Figure 3 illustrates that at x = 5, the surface of GaSb exhibits adhesion and increased roughness, indicative of corrosion products that have not been adequately complexed or decomposed. Consequently, despite the continued increase in oxidant concentration, the oxidation rate does not continue to rise and may even show a tendency to decrease. The optimal corrosion rate for GaSb is observed at a solution ratio of CrO_3: HF = 3:1.

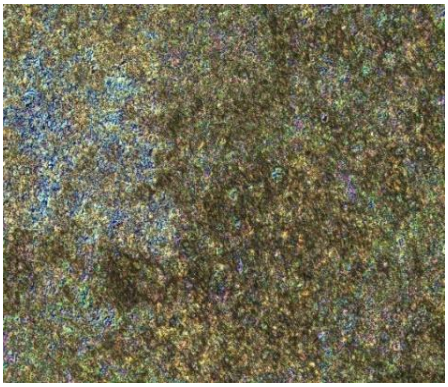

Figure 3: GaSb surface after corrosion at x=5

The study examined various ratios of corrosion solutions applied to InAsSb for a duration of five minutes, utilizing acetone and alcohol for the de-gumming process. Observations conducted under a metallurgical microscope revealed that both the exposed leakage area and the protected region exhibited only minimal traces of corrosion. Measurements of the height differential across each sample, obtained using a step meter, indicated a range of 40 to 50 nm. These findings suggest that the corrosion rate of the tested solutions on InAsSb is negligible and can be considered inconsequential.

Table 2: Corrosion rate of GaSb by solutions containing different amounts of chromium trioxide

Solution number	A	B	C	D	E
Corrosion rate nm/s	6.5	20.6	43.3	38.7	15.3

3.2. Effect of H_3PO_4 content on the corrosion rate of GaSb and InAsSb

H_3PO_4 is classified as a weak acid and serves as a corrosion complexing agent within the oxidative corrosion mechanism. This study examines the influence of varying concentrations of H_3PO_4 on the corrosion rates of GaSb and InAsSb, utilizing a specific C solution as the basis for experimentation.

The solution was prepared in the following ratio: CrO_3: HF: H_3PO_4 = 3:1: x, where x represents the concentrations of H_3PO_4 at 1.5, 2.5, 3.5, and 4.5. Initially, a predetermined amount of CrO_3 was weighed and added to a PTFE beaker, followed by the addition of a specific volume of water to facilitate dissolution. Upon complete dissolution, HF was incorporated and mixed thoroughly, after which H_3PO_4 was added and stirred uniformly to create the corrosion solution, designated as F, G, H, and I. Following the preparation of the solutions, they were allowed to stand for 10 minutes.

As illustrated in Figure 2, half of each material was protected with photoresist and subsequently baked at 90 ℃ for 10 minutes. The samples were then immersed in the various solution ratios for a duration of 5 minutes, after which they were rinsed in an overflow pool. The photoresist was removed using acetone and ethanol solutions, and the samples were dried with a nitrogen gun. Each material

was subjected to corrosion in three separate pieces for each solution ratio. A step meter was employed to measure the height difference between the exposed and protected areas, and the average height difference was calculated. This average was then divided by the corrosion time to determine the corrosion rate.

Table 3: Corrosion rate of GaSb by solutions containing different amounts of phosphoric acid

Solution number	F	G	H	I
Corrosion rate nm/s	58.6	98	173.4	156

As illustrated in Table 3, the corrosion rate of GaSb in the presence of H_3PO_4 initially increases with the concentration of H_3PO_4, followed by a subsequent decrease. The introduction of H_3PO_4 facilitates the complexation and oxidation processes involving HF, allowing for the timely decomposition and dissolution of oxidized products. This acceleration in the decomposition of oxidized materials subsequently enhances the oxidation of chromic acid. However, when the concentration of chromic acid becomes excessively high, it leads to a reduction in the overall concentration of chromic acid, which in turn diminishes the oxidation rate and results in a decrease in the corrosion rate.

In the case of InAsSb, after 5 minutes of exposure to the corrosion solution, measurements taken with a step meter indicated a height difference of 50-60 nm. This finding suggests that the corrosion rate of the solution on InAsSb is minimal and can be considered negligible.

3.3. Device Corrosion and Performance Testing

To assess the surface characteristics of the focal plane following corrosion and to evaluate any potential impact on its performance, a focal plane device was prepared with a residual substrate thickness of 25-30 μm after a single-point treatment. The substrate was subsequently subjected to corrosion and removal using an H solution. Figure 4 illustrates the morphology of the focal plane post-corrosion. A three-dimensional profiler was employed to examine the surfaces before and after the corrosion process. As depicted in Figures 5 and 6, the surface of the focal plane device exhibited a flat profile after corrosion, with surface roughness decreasing from S_a = 1.2853 nm prior to corrosion to S_a = 1.0679 nm afterward. This indicates that the application of the H solution results in a smoother and flatter surface.

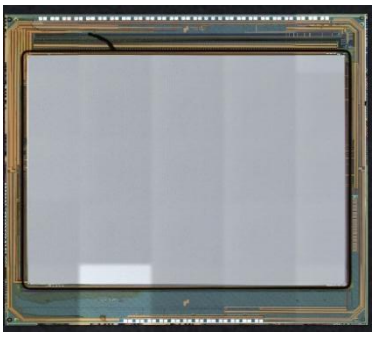

Figure 4: Morphology of the focal plane after corrosion

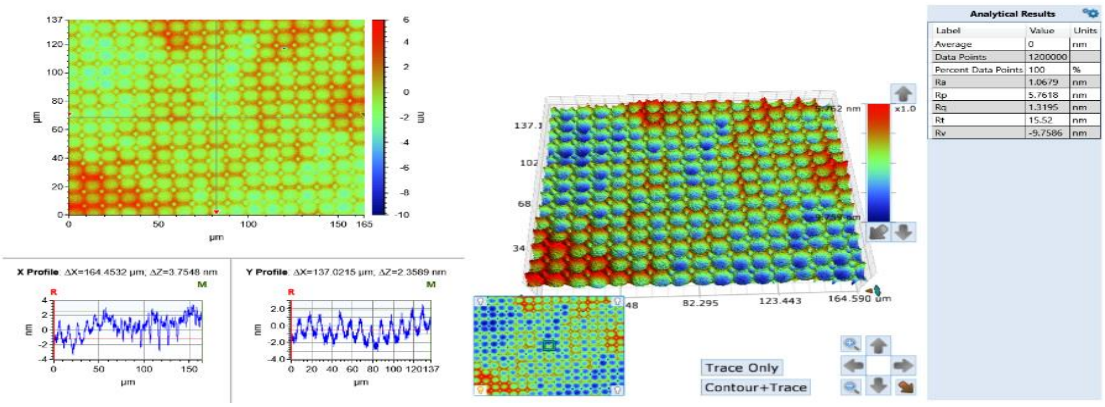

Figure 5: Surface morphology after corrosion

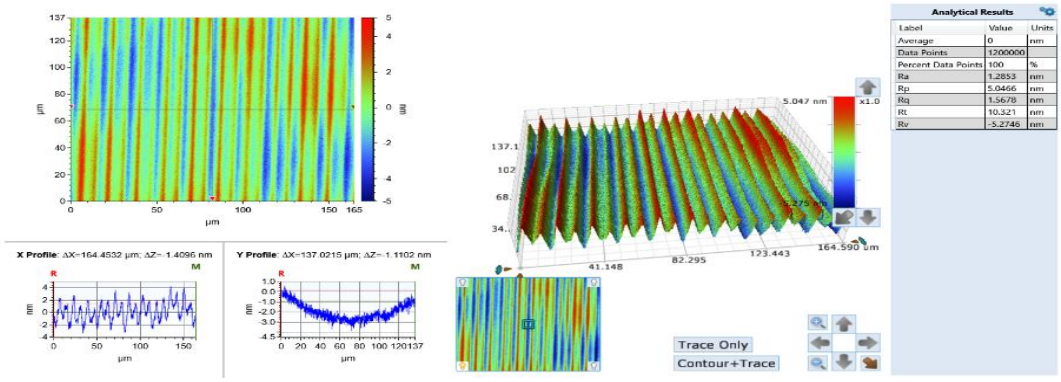

Figure 6: Surface morphology before corrosion

The corroded focal plane was prepared for testing Figure 7, with a target temperature of 25 ℃ for the blackbody and a testing temperature of 150 K. The results of the tests are presented in Table 4, indicating a blind element rate of 0.002% for the device, an average NETD value of 20.97 mK, and a voltage signal (Vs) of 553 mV. Furthermore, no damage was observed in the test level diagram, suggesting that the H-solution effectively mitigates damage caused by mechanical actions. The performance parameters of the focal plane device were found to be within the acceptable standard range, and the corrosion did not adversely affect the device's performance. These findings demonstrate that the H-solution is proficient in removing the substrate from the rear of the InAsSb focal plane device, thereby preventing the substrate from absorbing infrared radiation and enhancing the overall performance of the device.

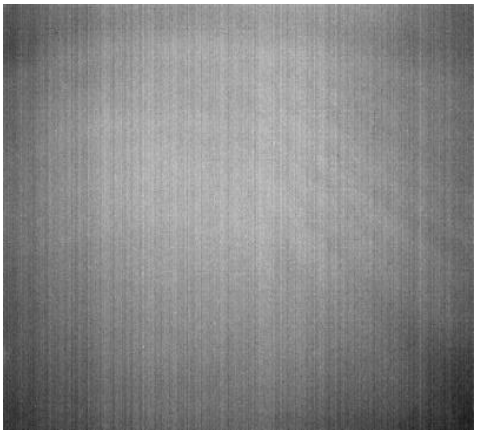

Figure 7: DC level diagram after back-reduced corrosion

Table 4: Detector test results

test item	in the end
Blind spot rate	0.002%
NETD	20.98mK
V_s	553mV
Response rate inhomogeneity	3.994%
response rate	$1.729E^{+9}$V/W

4. Conclusion

The investigation into the corrosion of GaSb and InAsSb materials, specifically in relation to the presence of CrO_3 and H_3PO_4 in the corrosion solution, yielded significant findings. The results indicate that an increase in the concentration of CrO_3 and H_3PO_4 within a certain range enhances the reaction rate of the solution. Furthermore, a corrosion solution composed of CrO_3, HF, and H_3PO_4 demonstrated the capability to completely eliminate the InAsSb focal plane substrate from GaSb. This corrosion solution exhibited high selectivity, a rapid corrosion rate, and resulted in minimal surface roughness post-corrosion, yielding a smooth surface devoid of abnormalities. Subsequent focal plane packaging tests revealed satisfactory performance parameters for the device, suggesting that the corrosion solution effectively removes the GaSb substrate without compromising the integrity of the focal plane device. These findings provide valuable insights into the methodology for the removal of the GaSb substrate.

References

[1] Yi C. Review and prospect of HgCdTe detectors[J]. Infrared and Laser Engineering, 2022, 51(1): 20210988.
[2] J. Piotrokski, A. Rogalski. High-Operation-Temperature Infrared Photodetectors[M].Bellingham: SPIE Press, 2007, 233-235.
[3] P.Martyniuk, A. Rogalski. HOT infrared photodetectors [J].Opto-Electron.Rev.2013, 21(2):239-257.
[4] Zhao Jun, Wang Xiaoxuan, Li Xiongjun, et al. Research progress of mercury cadmium telluride infrared detectors [J]. Science in China: Technological Science, 2023, 53(09):1419-1433
[5] J. Si. Novel infrared detector materials based on InSb (Invited)[J]. Infrared and Laser Engineering, 2022, 51(01):79-97.
[6] Deng Gongrong, Zhao Peng, Yuan Jun, et al. Research progress of antimony-based high operating temperature infrared detectors[J]. Infrared Technology, 2017, 39(09):780-784.
[7] Chen Dongqiong, Wang Haipeng, Qin Qiang, et al. Dark current characterization of InAsSb barrier-blocking infrared detectors[J]. Journal of Infrared and Millimeter Waves, 2022, 41(05):810-817.
[8] Chen Dongqiong, Yang Wenyun, Deng Gongrong, et al. Research progress of indium-arsenic-antimony infrared detectors [J]. Infrared Technology, 2022, 44(10):1009-1017.
[9] Li Chunling, Feng Xue, Xing Weirong, et al. Research on backside thinning technology for class II superlattice detectors[J]. Infrared, 2022, 43(09):10-14.
[10] Cheng Yu, Bao Yinghao, Xiao Yu, et al. Research on backside thinning technology of InAs/GaSb class II superlattice longwave infrared detectors[J]. Infrared, 2020, 41(08):15-20.
[11] Kang Zhe, Wen Tao, Guo Xi. Research on wet etching process of InAs/GaSb type II superlattice materials[J]. Laser and Infrared, 2018, 48(07):867-871.